# EXPERIMENTAL STUDY OF A HYBRID CNT/PCM STRUCTURE FOR THE TRANSIENT THERMAL MANAGEMENT OF ELECTRONICS

Kinkelin C.[1]*, Lips S.[1], Lefèvre F.[1], Soupremanien U.[2], Remondière V.[2], Dijon J.[2], Le Poche H.[2], Ollier E.[2], Zegaoui M.[3], Rolland N.[3], Rolland P-A.[3], Lhostis S.[4], Descouts B.[4] and Kaplan Y.[5]
*Author for correspondence
[1]CETHIL UMR5008, University of Lyon, CNRS, INSA-Lyon,
[2]CEA Liten, [3]IEMN, [4]STMicroelectronics, [5]Kaplan Energy,
[1,2,3,4,5]France,
E-mail: christophe.kinkelin@insa-lyon.fr

## ABSTRACT

A Thermal Interface Material with Thermal Storage capacity (TIM-TS) consisting mainly of a carbon nanotubes (CNT) array filled with phase change material (PCM) and integrated between two silicon chips is experimentally studied by means of a heating laser and an infrared camera in order to characterize its thermal behavior. The TIM-TS is intended to smooth temperature peaks of transient electronic components as a result of the high latent heat of the embedded PCM while keeping a high global thermal conductance thanks to the CNT array linking its two silicon chips. These two thermal properties are estimated thanks to the measured thermal response of different TIM-TS prototypes. A decrease of 5 K of the maximum TIM-TS temperature is measured with a mass fraction of PCM as low as 2.4%. The qualitative estimation of the thermal contact resistances at the CNT/silicon interfaces enables to identify the location of the major thermal resistance for the tested samples.

## NOMENCLATURE

| | | |
|---|---|---|
| *a, b, g* | [-] | Coefficients |
| *c* | [$J.kg^{-1}.K^{-1}$] | Specific heat |
| *G* | [$W.K^{-1}$] | Global thermal conductance |
| *m* | [kg] | Mass |
| $\dot{Q}_{abs}$ | [W] | Part of the laser heat flux absorbed by the sample |
| $R_{mes}$ | [$W.sr^{-1}.m^{-2}$] | Radiance measured by the IR camera |
| $R^0$ | [$W.sr^{-1}.m^{-2}$] | Black body radiance |
| *T* | [°C] | Temperature |
| Special characters | | |
| *α, β, γ* | [-] | Coefficients |
| Subscripts | | |
| *Air* | | related to sample "Air" |
| *amb* | | ambient |
| *bSi* | | behind silicon |
| *CNT* | | related to the CNT array |
| *do* | | downstream |
| *eq* | | equivalent |
| *m* | | spatial mean value |
| *PCM* | | related to sample "PCM" |
| *Si* | | silicon |
| *stp* | | stamping layer |
| *up* | | upstream |

## INTRODUCTION

The running miniaturization and the increasing performance of electronic devices lead to higher power densities and higher integration of electronic components with 3D packaging instead of 2D arrangements. For electronic components experiencing intermittent solicitations, these overall higher heat fluxes bring higher temperature peaks. The maximal allowable chip temperature of various electronic components generally ranges between 85°C and 120°C [1]. Exceeding this maximum temperature can reduce the performance and shorten the lifetime of the electronic component. Transient electronic components are used in various applications like telecommunications and transportations. It is of interest to develop passive transient thermal management solutions in order to smooth the chip temperature.

Phase Change Materials (PCMs) can store a large amount of energy at almost constant temperature thanks to their high latent heat of fusion or solidification. Examples of PCMs are paraffin waxes, fatty acids and sugar alcohols. They are used in various applications like thermal storage of solar energy, passive thermal regulation of buildings, thermal protection of biological products or food and electronic thermal management [2, 3]. They are a passive, light and simple solution to manage transient heat dissipation in electronic devices. Nevertheless, PCMs generally exhibit a low thermal conductivity. This is a drawback for applications needing a fast melting/freezing of the PCM and for the studied TIM-TS because the heat flow from the electronic component to the cold source is supposed to cross the PCM area.

Thermal conductivity enhancement through introduction of high-conductivity nanostructures into PCMs (carbon-based nanostructures, carbon nanotubes, metallic and metal oxide nanoparticles and silver nanowires) leads to an effective thermal conductivity up to only two times higher than the thermal conductivity of PCMs [4]. The thermal conductivity of such composite PCMs remains small because of the high thermal resistance between neighboring high-conductivity elements. A much better thermal conductivity enhancement is reported when a thermal link exists between the particles, thus forming a single non-moving conductive matrix like graphite nanofibers with controlled graphite plane orientation [5] or a graphite matrix [6].

In the field of electronics, the most recent studies on passive cooling with PCM are relatively basic. PCM can be embedded between the fins of a traditional heat sink [1, 7, 8] or between high conductivity carbon walls with CNTs added into the PCM [9]. PCM integration in an array of micro-reservoirs etched in a silicon substrate in order to stabilize the surface temperature during short transient thermal solicitations is also reported, but the areal thermal energy storage density remained small [10].

Advanced thermal management techniques are developed for CNT-based TIMs (thermal interface materials) in order to profit from the very high individual thermal conductivity of CNTs. TIMs are used to minimize the thermal contact resistance between two components but they have no heat storage function. The overall thermal conductance of TIMs consisting of vertically aligned CNT arrays can be significantly improved by the penetration of the CNT array into the mating surface [11], for example by bonding the free-end CNT tips into an indium sheet [12]. These findings show the importance of the thermal transfer between the CNTs and the partner surfaces for the overall thermal conductance.

The TIM-TS presented in this paper aims at smoothing the temperature peaks of transient electronic components while maintaining a high thermal conductance through its structure. The TIM-TS consists mainly of vertically aligned carbon nanotubes (CNT) and phase change material (PCM) embedded in a silicon box (figure 1). It is located between the hot source (electronic chip) and the cold source (e.g. Printed Circuit Board).

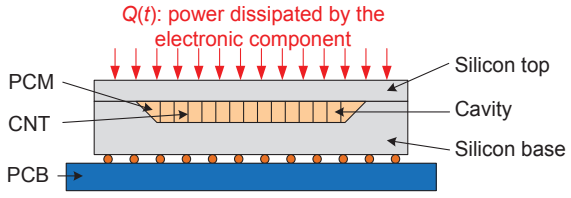


**Figure 1**. Cross-section view of a TIM-TS.

The low thermal conductivity of most PCMs implies the use of a high conductivity matrix of CNT. The carbon nanotubes enhance both the heat transfer from the hot side to the cold side of the TIM-TS and the heat transfer rate between the conductive structure and the PCM. The mating surfaces of the CNT array are a catalyst layer at one end and a stamping layer at the other end.

In this study, different samples are tested in order to estimate some important thermal parameters like the latent heat of fusion, the temperature smoothing effect and the relative importance of the interfacial thermal resistances at the CNT/silicon contacts.

## EXPERIMENTAL SETUP

The test bench is inspired by the flash method and consists mainly of an enclosure, a laser and an infrared (IR) camera (figure 2).

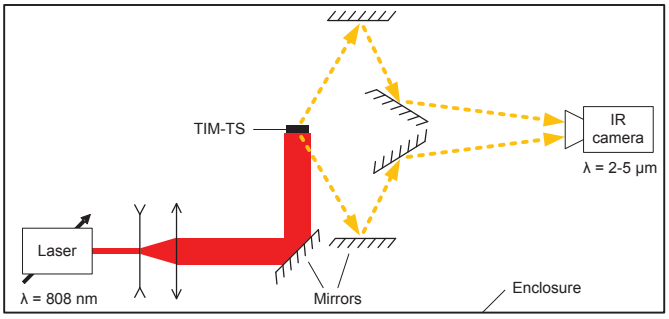


**Figure 2.** Optical layout of the test bench.

The 808 nm laser (nLight Pearl TKS) enables a non-invasive heating of one side of the TIM-TS. The silicon of the TIM-TS is optically thick at this wavelength. The laser output power can be time modulated between 0 and 30 W, thus allowing laser flash measurement or longer solicitations like crenel- or sinus-type signal. The laser beam is expanded via a set of lenses and directed toward the TIM-TS via a high reflectance mirror.

Both sides of the TIM-TS are simultaneously visualized by the infrared camera by means of a set of infrared mirrors. The infrared system (FLIR SC7600) is sensible from 2.5 to 5.5 µm wavelength. Silicon is semi-transparent in this wavelength range.

In order to measure the surface temperature of the TIM-TS, dull black opaque paint can be applied. The drawbacks of painting the sample are additional thermal inertia and thermal resistance due to the paint layer of about 60 µm thick.

The voluminous light tight enclosure maintains a controlled radiative environment as well as a constant air temperature around the TIM-TS. The sample is hold in the laser beam by three thin metallic rods with a V-shape end (figure 3).

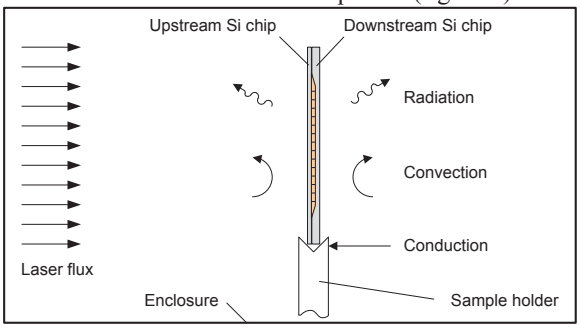


**Figure 3**. Thermal boundary conditions for the TIM-TS.

### Test samples

Two thermal properties are studied in this paper, corresponding to two different couples of samples. These samples were produced within a collaborative project by the following partners: CEA-Liten, IEMN, Kaplan Energy and STMicroelectronics [13].

Firstly, the temperature smoothing effect of the PCM is estimated by comparison of one sample with PCM and one sample without PCM (figure 4a). The PCM used in this study is a paraffin wax with a carbon distribution of C30 to C48 (PCM-

89 from Kaplan Energy) and has a latent heat of fusion of 205 kJ/kg. Black paint is applied on two corners per sample's face in order to simultaneously measure the temperature of both sides and visualize the behavior of the PCM inside the cavity through the unpainted silicon (figure 4b).

a)

| | TIM-TS | | | Cavity | | | |
|---|---|---|---|---|---|---|---|
| Name | Area | Thickness | Mass | Area | Depth | PCM | CNT |
| PCM | 20 x 20 mm$^2$ | 760 µm | 674 mg | 16 x 16 mm$^2$ | 149 µm | yes | no |
| Air | | | | | 101 µm | no | |

b)

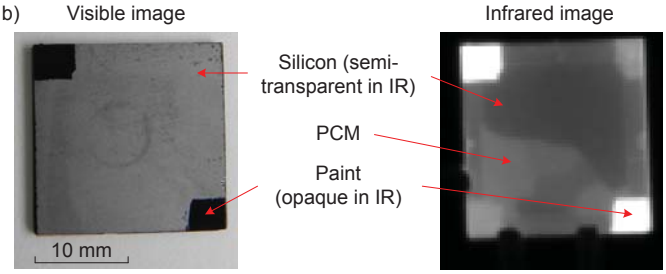


**Figure 4.** Samples for the temperature smoothing study. a) Specifications. b) Images of the "PCM" sample.

Secondly, the thermal contact resistances at the interfaces between silicon and CNTs are estimated with two samples containing CNTs (figure 5a).

a)

| | TIM-TS | | | Cavity | | |
|---|---|---|---|---|---|---|
| Name | Area Si-Bottom | Area Si-Top | Thickness | Depth | PCM | CNT |
| CNT-A | ~ 15 x 15 mm$^2$ | ~ 10 x 10 mm$^2$ | 1200 µm | 100 µm | no | yes |
| CNT-P | | | | | yes | |

b)

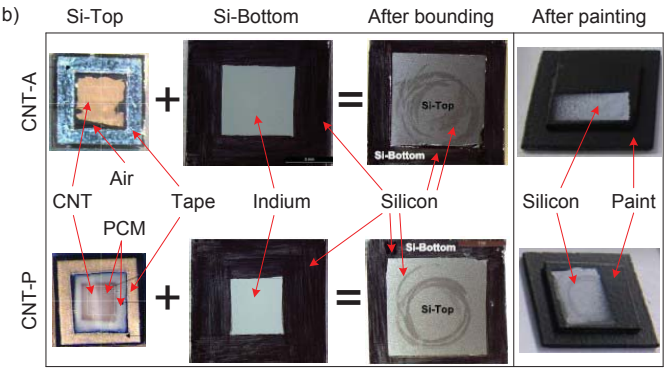


**Figure 5.** Samples for the contact resistance study. a) Specifications. b) Pictures of the inside and outside.

These samples are preliminary prototypes and exhibit therefore a less even shape than the ones described above. CNTs are first vertically grown until a length of circa 100 µm on a thin iron (Fe) catalyst layer covering the "Si-Top" chip. Then 20 nm of titan (Ti) and 100 nm of gold (Au) are deposited on the CNTs. Adhesive tape is applied around the CNTs. PCM is melted on the CNTs of the "CNT-P" sample only. The whole Si-Top chip is pressed against the Ti/Au/Indium layer (20 / 100 / 500 nm) of the "Si-Bottom" chip. Both samples are painted on both sides except an IR visualization window on the Si-Top chips (figure 5b).

## TEMPERATURE SMOOTHING EFFECT OF THE PCM

### TIM-TS response to a crenel-type solicitation

The mean temperature $T_m$ of the TIM-TS is defined as the mean value of the temperatures of the upstream and downstream chips weighted by their respective masses, the other masses (PCM, thin layers, paint) being neglected:

$$T_m = \frac{m_{up}T_{up} + m_{do}T_{do}}{m_{up} + m_{do}} \quad (1)$$

$T_{up}$ and $T_{do}$ are the mean values of the temperatures measured on the painted corners of the upstream and the downstream sides of the sample respectively.

The "Air" sample has a less deep cavity in order to compensate the absence of PCM so that both "Air" and "PCM" samples have the same mass (figure 4). Figure 6 shows the influence of PCM on the temperature response of the TIM-TS to an 18 s long crenel-type laser solicitation. The laser power absorbed by the TIM-TS is about 3 W. Despite the low mass fraction of PCM in this prototype "PCM" sample (2.4%), the decrease of the maximum TIM-TS temperature is about 5 K in comparison to the "Air" sample.

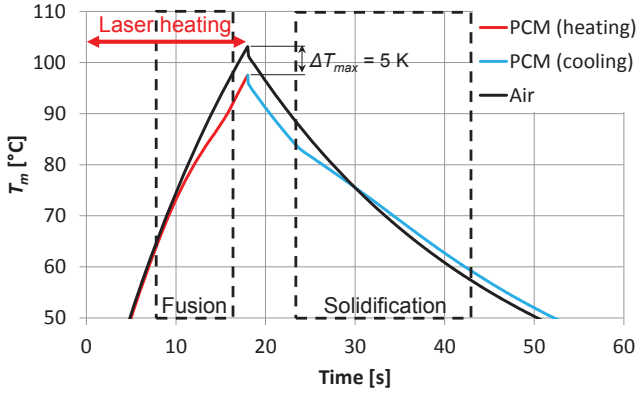


**Figure 6.** Temperature smoothing effect of the PCM.

The derivative of $T_m$ with respect to time versus $T_m$ allows to clearly identify the temperature domains in which phase change occur (figure 7). Before the laser crenel, both samples are at ambient temperature (null derivative). After the start peak corresponding to the establishment of the temperature gradient between the paint and the silicon of the upstream chip, both samples exhibit a similar heating rate until the PCM starts to melt around 64°C. The melting of PCM absorbs energy, thus slowing down the temperature increase of the "PCM" sample until the end of fusion at a temperature of about 91°C. Then the heating rates of both samples are again the same until the end of the laser crenel.

Likewise, the cooling rates of both samples differ only during the freezing of the PCM between 84°C and 60°C. The start of freezing occurs at a 7 K lower temperature than the end of fusion and is due to supercooling of the PCM.

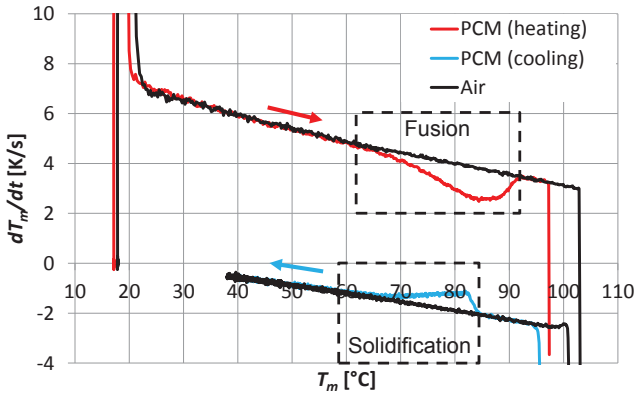


**Figure 7.** Thermal signatures of "Air" and "PCM" samples.

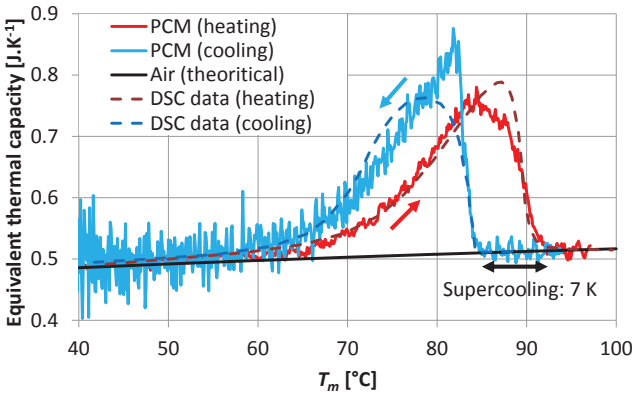


**Figure 8.** Experimental thermal capacities of "PCM" sample versus DSC measurements.

**Estimation of the PCM mass**

The mass of embedded PCM is estimated by processing the temperature profiles shown in figure 6. Following assumptions are made about the TIM-TS located in the test bench (figure 3):

- The sample temperature is uniform and equal to $T_m(t)$.
- The temperature of the ambiance (air, enclosure walls, sample holders) $T_{amb}$ is constant.
- The convective, radiative and conductive heat transfer modes between the sample and its environment are described by a global thermal conductance $G(T_m)$ depending only on $T_m$ and not on the time.

Thus the energy balance of the TIM-TS is:

$$\dot{Q}_{abs} - G \cdot (T_m - T_{amb}) = (mc)_{eq} \frac{dT_m}{dt} \qquad (2)$$

with $\dot{Q_{abs}}$ being the laser flux absorbed by the sample and $(mc)_{eq}$ the equivalent thermal capacity of the sample including the sensible and latent heats of the PCM.

For a given sample temperature $T_m$, the "PCM" and "Air" samples absorb the same fraction of laser incident power $\dot{Q_{abs}}$ because their external dimensions and their state of surface are similar. Likewise, for a given temperature $T_m$, the cooling heat flux between the TIM-TS and its environment $G \cdot (T_m - T_{amb})$ depends only on $T_m$ and is therefore similar for both samples.

For a given sample temperature $T_m$, it turns to:

$$(mc)_{eq,PCM} \frac{dT_{m,PCM}}{dt} = (mc)_{eq,Air} \frac{dT_{m,Air}}{dt} \qquad (3)$$

One can estimate the equivalent thermal capacity of the "PCM" sample $(mc)_{eq,PCM}$ thanks to the measured derivatives (figure 7), the measured mass $m$ of the "Air" sample and its specific heat $c$, here considered equals to the one of pure silicon. Figure 8 shows the estimated equivalent thermal capacity of the "PCM" sample as well as the considered one of the "Air" sample. They are similar out of the phase change temperature range. Results for the PCM-89 measured alone by Kaplan Energy on a Differential Scanning Calorimetry (DSC) apparatus are also displayed in figure 8. DSC measurements are very close to the thermal capacities estimated in this study. The supercooling effect is similar for both cases.

As for a DSC analysis, a baseline corresponding to the thermal capacity that the sample would have without the latent heat contribution can be calculated. In figure 8, it would be similar to the curve of the "Air" sample. Integrating the difference between the thermal capacity of the "PCM" sample and its baseline gives the latent heat of phase change. Estimated latent heat of fusion and solidification are 3.27 J and 3.32 J respectively, corresponding to an estimated mass of PCM of 15.9 mg and 16.2 mg respectively.

## ESTIMATION OF THE THERMAL INTERFACIAL RESISTANCES

The major thermal resistances in the TIM-TS are located at the interfaces between the CNT array and the silicon chips. In this part, the "CNT-P" and "CNT-A" samples are tested with the optical setup described in figure 2. The evolutions of the IR radiations emitted from both sides of the samples are analyzed in order to find out which interface (stamping or catalyst layer) controls the heat flux from the upstream to the downstream silicon chip.

**Signal measured by the IR camera**

The different contributions to the signal measured by the IR camera are detailed below. The atmospheric attenuation is neglected since the optical distance between the sample and the IR camera is short (1.2 m). The silicon is semi-transparent in the wavelength range of the IR camera (2.5-5.5 µm). Thus, the radiance measured by the IR camera $R_{mes}$ is the sum of:

- the radiance emitted by the filmed silicon chip,
- the transmitted radiance of the objects behind this silicon chip and
- the reflection of the environment contribution on the TIM-TS (figure 9).

It can be written as:

$$R_{mes} = aR^0(T_{Si}) + bR^0(T_{bSi}) + gR^0(T_{amb}) \qquad (4)$$

with a, b and g three coefficients varying between 0 and 1.

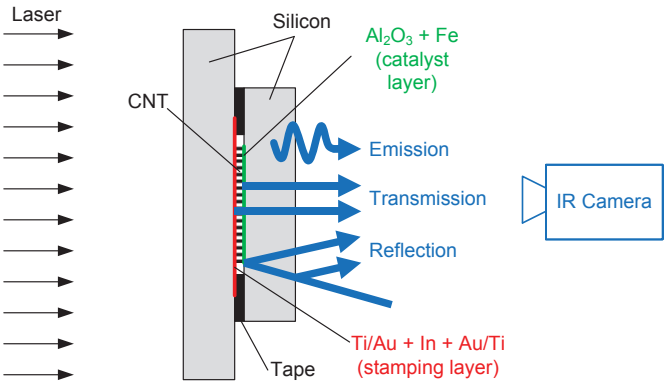


**Figure 9**. Schematic illustration of the contributions to the infrared signal measured by the IR camera.

Preliminary measurements showed that the stamping layer (Ti/Au/In/Au/Ti) and the CNT array are opaque whereas the catalyst layer is semi-transparent in the 2.5-5.5 µm range. The contact between the stamping layer and the silicon substrate is assumed as perfect ($T$ [illegible]) since it was deposited by PVD. The IR signal of the unpainted samples acquired in the central region delimited by the CNT array can be expressed as follow for the upstream side:

[illegible] (5)

Likewise, the measured radiance from the central zone of the downstream side of the TIM-TS is:

[illegible] (6)

The signal measured by the IR camera is expressed in digital level (DL) and is proportional to the radiance.

**Interfacial resistance at the stamping layer**

A 10 ms laser flash is delivered to the large silicon chip of the unpainted samples "CNT-P" and "CNT-A", as schematized in figure 9. The samples are at ambient temperature before the flash.

The radiance evolution of the upstream side $R_{mes,up}$ is similar for both samples (figure 10). The quick increase of radiance during the flash corresponds to a quick increase of the temperature of the upstream silicon chip $T_{Si,up}$.

The radiance of the downstream side of the "CNT-P" sample (figure 11) increases almost simultaneously with the radiance of its upstream silicon chip (figure 10). $T_{amb}$ being constant implies that $T_{Si,do}$ and/or $T_{CNT}$ (6) increase almost simultaneously with $T_{Si,up}$ (5). Considering the thicknesses and the thermal properties of the silicon and the tape, heat flowing from the upstream to the downstream silicon chip through the tape would need much more time to induce an increase of $T_{Si,do}$ and even more so of $T_{CNT}$. This implies that the heat flows directly from the upstream silicon chip to the CNT array through the stamping layer. The almost simultaneous increase of $T_{CNT}$ and $T_{Si,up}$ corresponds to a very low thermal interfacial resistance at the stamping layer for the "CNT-P" sample.

The sample "CNT-A" exhibits a much slower radiance increase of its downstream side than the "CNT-P" sample (figure 11). This implies a high thermal interfacial resistance at the stamping layer for the "CNT-A" sample.

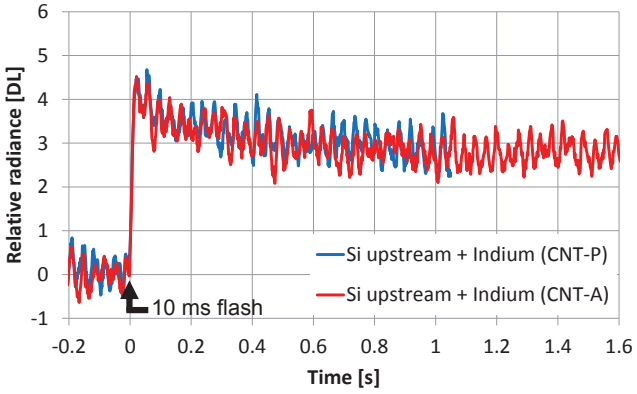


**Figure 10.** IR radiation of the upstream silicon and the stamping layer $R_{mes,up}$ of unpainted samples "CNT-P" and "CNT-A"

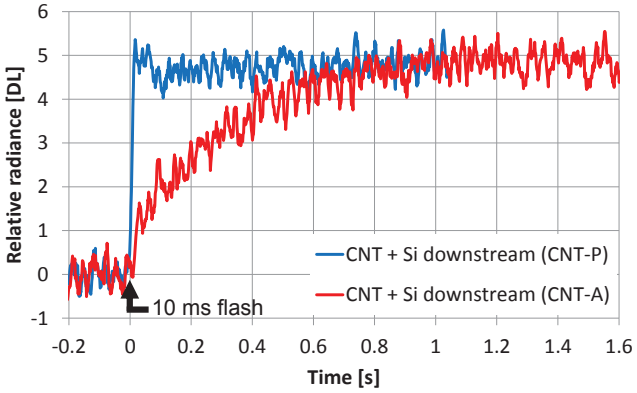


**Figure 11.** IR radiation of the downstream silicon and the CNT array $R_{mes,do}$ of unpainted samples "CNT-P" and "CNT-A"

**Interfacial resistance at the catalyst layer**

The samples "CNT-P" and "CNT-A" are then tested after painting (figure 5). The thermal solicitation is still a 10 ms laser flash directed toward the large painted silicon chip.

The measurement of the CNT area through the IR visualization window shows the same thermal behavior as the one described in figure 11.

The known emissivity of the paint enables to convert the measured radiance of the paint into temperature. The temperature increase of the downstream paint and thus of the downstream silicon chip of the "CNT-P" sample (figure 12) is much slower than the temperature increase of its CNT array. This implies a high interfacial thermal resistance at the catalyst layer of the "CNT-P" sample.

The very similar temperature profile of the downstream silicon chip of both "CNT-P" and "CNT-A" samples (figure 12) let think that the tape is the controlling thermal resistance of both samples. In that case, the interfacial thermal resistances of the catalyst layer of the "CNT-P" sample and of the stamping layer of the "CNT-A" sample would be much higher than the thermal resistance of the tape, thus leading to the observed similar global thermal resistance for both samples.

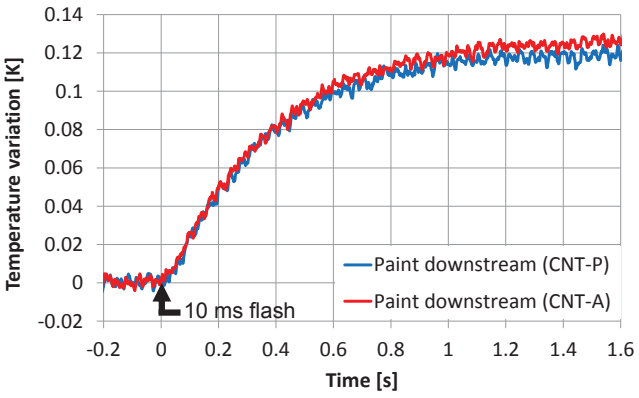


**Figure 12.** Temperature profile of the paint of the downstream silicon chip.

## CONCLUSION

The thermal behavior of a new hybrid CNT/PCM structure was experimentally studied by means of an infrared thermography system and a heating near-visible laser. The studied hybrid structure is embedded between two silicon chips and is intended to smooth the temperature peaks of transient electronic components. The thermal conductivity of the PCM being low, the CNT array linking both silicon chips is supposed to ensure a high thermal conductance through the TIM-TS as well as in the PCM itself.

A first set of TIM-TS samples (one with and one without PCM) shows a lowering of 5 K of the maximum temperature with a mass fraction of PCM as low as 2.4%. A mass fraction of PCM of 10% or more should be easily reachable for industrial grade TIM-TS with a larger cavity, which would bring a much more significant smoothing effect.

A second set of prototypes containing CNTs was tested first without and then with paint in order to qualitatively estimate the thermal interfacial resistance at both ends of the CNT array. The thermal contact resistance at the stamping interface is very low for the "CNT-P" sample and high for the "CNT-A" sample. The thermal contact resistance at the catalyst layer could be estimated for the "CNT-P" sample and it is high. The implementation of two stamping interfaces with very low thermal contact resistance at both ends of the CNT array could lead to a very high global thermal conductance in future samples. As a next step, a numerical model of the TIM-TS in combination with experimentally estimated parameters will enable the determination of optimal designs of the hybrid CNT/PCM structure depending on the applications.

## ACKNOWLEDGEMENTS

This project was carried out in collaboration with the CEA-Liten, the IEMN, Kaplan Energy and STMicroelectronics. It was supported by the ANR P2N "THERMA3D" project N°ANR-11-NANO-011.

## REFERENCES

[1] R. Kandasamy, X.-Q. Wang, et A. S. Mujumdar, « Transient cooling of electronics using phase change material (PCM)-based heat sinks », *Appl. Therm. Eng.*, vol. 28, n° 8‑9, p. 1047‑1057, juin 2008.

[2] B. Zalba, J. M. Marín, L. F. Cabeza, et H. Mehling, « Review on thermal energy storage with phase change: materials, heat transfer analysis and applications », *Appl. Therm. Eng.*, vol. 23, n° 3, p. 251‑283, févr. 2003.

[3] S. S. Anandan et V. Ramalingam, « Thermal management of electronics: A review of literature », *Therm. Sci.*, vol. 12, n° 2, p. 5–26, 2008.

[4] J. M. Khodadadi, L. Fan, et H. Babaei, « Thermal conductivity enhancement of nanostructure-based colloidal suspensions utilized as phase change materials for thermal energy storage: A review », *Renew. Sustain. Energy Rev.*, vol. 24, p. 418–444, 2013.

[5] R. D. Weinstein, T. C. Kopec, A. S. Fleischer, E. D. Addio, et C. A. Bessel, « The Experimental Exploration of Embedding Phase Change Materials With Graphite Nanofibers for the Thermal Management of Electronics », *J. Heat Transf.*, vol. 130, n° 4, p. 040301.1‑044503.4, 2008.

[6] A. Mills, M. Farid, J. R. Selman, et S. Al-Hallaj, « Thermal conductivity enhancement of phase change materials using a graphite matrix », *Appl. Therm. Eng.*, vol. 26, n° 14, p. 1652–1661, 2006.

[7] X.-Q. Wang, A. S. Mujumdar, et C. Yap, « Effect of orientation for phase change material (PCM)-based heat sinks for transient thermal management of electric components », *Int. Commun. Heat Mass Transf.*, vol. 34, n° 7, p. 801‑808, août 2007.

[8] G. Setoh, F. L. Tan, et S. C. Fok, « Experimental studies on the use of a phase change material for cooling mobile phones », *Int. Commun. Heat Mass Transf.*, vol. 37, n° 9, p. 1403‑1410, nov. 2010.

[9] S. Shaikh et K. Lafdi, « C/C composite, carbon nanotube and paraffin wax hybrid systems for the thermal control of pulsed power in electronics », *Carbon*, vol. 48, n° 3, p. 813–824, 2010.

[10] C. Muratore, S. M. Aouadi, et A. A. Voevodin, « Embedded phase change material microinclusions for thermal control of surfaces », *Surf. Coat. Technol.*, vol. 206, n° 23, p. 4828–4832, 2012.

[11] J. Xu et T. S. Fisher, « Enhancement of thermal interface materials with carbon nanotube arrays », *Int. J. Heat Mass Transf.*, vol. 49, n° 9, p. 1658–1666, 2006.

[12] T. Tong, Y. Zhao, L. Delzeit, A. Kashani, M. Meyyappan, et A. Majumdar, « Dense vertically aligned multiwalled carbon nanotube arrays as thermal interface materials », *Compon. Packag. Technol. IEEE Trans. On*, vol. 30, n° 1, p. 92–100, 2007.

[13] E. Ollier, U. Soupremanien, V. Remondière, J. Dijon, H. Le Poche, F. Lefevre, S. Lips, C. Kinkelin, N. Rolland, P. A. Rolland, M. Zegaoui, S. Lhostis, P. Ancey, B. Descouts, et Y. Kaplan, « Thermal management of electronic devices by composite materials integrated in silicon », in *Microtherm*, Lodz, Poland, 2013.